Journal of Sound and Vibration (2002) **252**(4), 717–727
doi:10.1006/jsvi.2001.3697, available online at http://www.idealibrary.com on IDEAL®

FINITE ELEMENT MODEL UPDATING USING ANTIRESONANT FREQUENCIES

K. JONES

Propulsion Directorate, Air Force Research Laboratory, 1950 *Fifth Street, Wright Patterson AFB, OH* 45433-7251, *U.S.A.*

AND

J. TURCOTTE

Air Vehicles Directorate, Air Force Research Laboratory 2130 *Eighth Street, Wright Patterson AFB, OH* 45433-7542, *U.S.A.*

(*Received* 28 *November* 2000, *and in final form* 23 *March* 2001)

This paper uses antiresonant frequencies in the finite element model updating of an experimental 6-m aluminum truss and analyzes the physical correctness of the updated model by using it to detect damage. Rigid elements are used to simplify the modelling of welded joints, and their dimensions are used as parameters in an iterative update based on eigenvalue and antiresonance sensitivities. An update using both natural frequencies and antiresonant frequencies is shown to produce a 48% better correlation to experimental frequency response functions (FRFs) than an update that uses only natural frequencies. The antiresonant updated model is used to predict FRFs for the truss in 112 damaged configurations. Pattern classification and curve-fit algorithms for damage detection are tested. The curve-fit method correctly identified damage 92·6% of the time compared to 76·1% for the pattern classifier. The high quality of the model is attributed to the use of rigid elements that are updated using antiresonant frequencies.

1. INTRODUCTION

After compiling a comprehensive literature survey and authoring a textbook on finite element (FE) model updating, Friswell and Mottershead concluded that the current state of the art in FE model updating involves using natural frequencies and possibly mode shape sensitivities [1]. However, the use of mode shape sensitivities entails three major difficulties. (1) Measured mode shapes are usually accurate to within 10% at best [1]. (2) Measured mode shapes must either be expanded to the number of degrees of freedom (d.o.f.) in the FE model (using the not-yet-updated FE model) or the FE model must be reduced to the number of measured d.o.f., both of which increase error in either the mode shape data or the FE model. (3) The calculation of mode shape sensitivities is difficult compared to natural frequency sensitivities [2]. Mode shapes are often used despite these problems, because the ability of model updating to converge on unique parameters is largely dependent on the amount of measured data available [3].

In 1999, Mottershead concluded that using antiresonant frequencies in model updating can be a preferred alternative to using mode shape data [4]. The motivation for using antiresonant frequencies in updating is that, unlike mode shapes, they are easily and accurately measured. Mottershead also showed that antiresonance sensitivities can be

0022-460X/02/$35.00

expressed as a linear combination of eigenvalue and mode shape sensitivities. Therefore, antiresonant frequencies do not offer the model updating process any new independent information over the natural frequencies and mode shapes commonly used in model updating. However, measured antiresonant frequencies can serve as a more accurate replacement for measured mode shape data.

Lallement and Cogan [5] and Rade *et al.* [3] have applied antiresonant frequency data to FE model updating and shown its potential benefits. Rade *et al.* demonstrated their method with a numerical example of a free–free uniform beam. To the authors' knowledge, antiresonant frequency data have not been applied to the model updating of an experimental structure in the published literature. The goal of this research was to demonstrate FE model updating using antiresonant frequencies on an experimental structure, compare the method to model updating that uses only natural frequencies, and analyze the physical correctness of the model by using it to detect damage. The ability to correctly model damaged states of the structure (states which were not involved in the updating process) was chosen to be an indicator of the physical correctness of the model and the success of model updating using antiresonant frequencies.

2. EXPERIMENTAL SET-UP

FE model updating using antiresonant frequencies was applied to the modelling of the Air Force Institute of Technology (AFIT) 6-m flexible truss experiment (FTE). The FTE is a vertically cantilevered 6-m truss. The assembled truss has a square cross-section of 50 cm. It has four vertical square cross-section aluminum longerons that run the length of the frame. The longerons are connected by aluminum square cross-section horizontal battens which divide the FTE into eight bays. Each bay has four tubular bolt-in Lexan diagonal members arranged to create a back-to-back "K" pattern over the FTE. Figure 1 is a diagram of the experimental set-up.

Although the FTE is called a truss, its connections are not pinned but bolted and welded. The FTE diagonals are bolted to vertical plates which are welded to battens and longerons. These connections are referred to as *vertical plate joints* and are shown in Figure 2. In

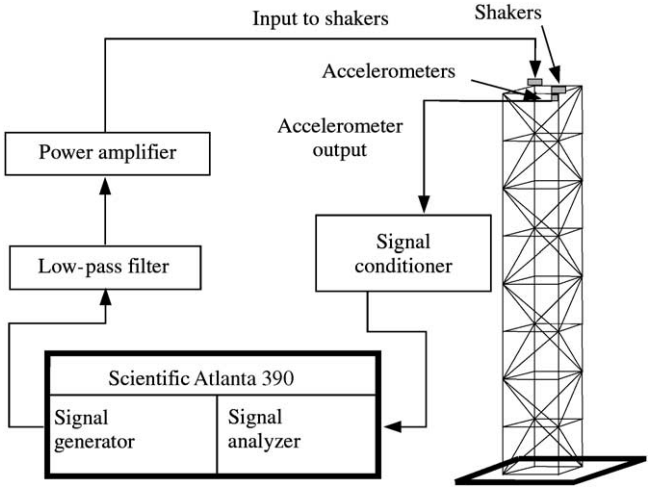

Figure 1. Experimental set-up.

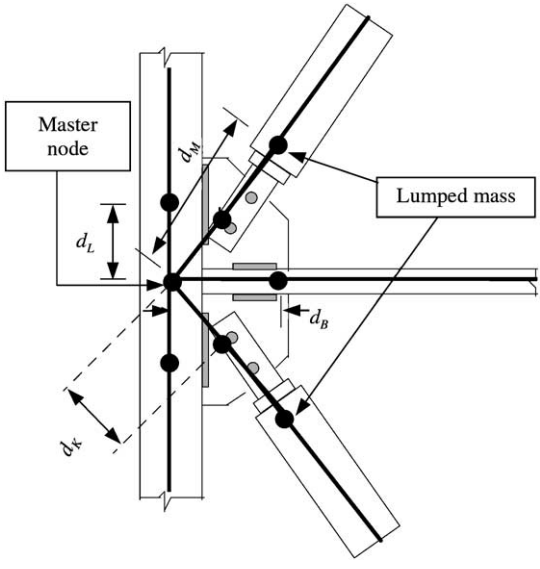

Figure 2. Vertical plate mesh. All nodes rigidly attach to the master node.

addition, small triangular horizontal plates welded to the longerons and battens are present in the joints at the top and mid-height of the FTE. These joints are referred to as *top-plate joints* and *mid-plate joints* respectively. Finally, the locations where battens are welded to longerons, but no diagonals are present, are referred to as *regular batten joints*.

Two electromagnetic shakers were used at the top of the truss to simultaneously excite the structure in two orthogonal lateral directions. Pseudo-random white noise was generated as input to the shakers while eight accelerometers, four at mid-height and four at the free end, measured the response. The accelerometers were aligned in the same orientation as the shakers and orthogonal to each other.

3. FINITE ELEMENT MODEL DEVELOPMENT

The Structural Dynamics Toolbox™ (SDT) for MATLAB™ [6] was used to create an FE model of the FTE. The standard 12-d.o.f. beam element was used to model all members of the FTE.

The complicated combinations of bolted and welded connections in the FTE joints were difficult to accurately model. Previous researchers [7, 8] had difficulty obtaining an accurate FE model of the FTE even after model updating, due to errors in modelling the joints. Rigid elements were chosen to model the FTE joints in this research. This method was chosen based on the successful use of rigid elements to parameterize and update joints by Mottershead *et al.* [9], Ahmadian *et al.* [10], and Horton *et al.* [11]. Rigid elements were particularly useful, because they did not add d.o.f.s to the model. The final model used 248 nodes but only had 192 d.o.f. due to the constraints applied by rigid elements.

The vertical plate joints were modelled using rigid elements as shown in Figure 2. One rigid element was used to place a lumped mass, representing the heavy solid aluminum end of the diagonal, in its realistic position. The placement of these diagonal end masses was critical to accurately model the torsional modes of the FTE. Another rigid element was used to connect the diagonal beam element to the master node. The variables d_L, d_M, d_B and d_K in

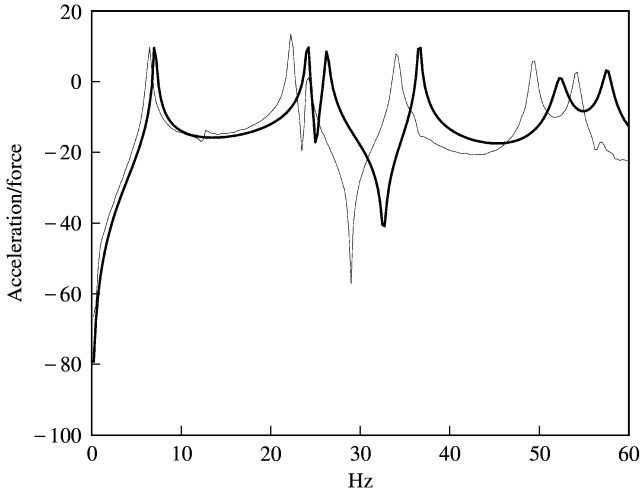

Figure 3. FRF correlation from initial model: ——, modelled; ——, experimental.

Figure 2 stand for the dimensions of the rigid elements that connect the longeron, lumped mass, batten and diagonal element. Other joints were modelled similarly with parameters d_{RB}, d_{MP} and d_{TP} standing for the dimensions of the rigid elements in *regular batten*, *mid-plate* and *top-plate* joints respectively.

Initial values were chosen for the joint parameters based on the geometry of the joints. The initial correlation between a modelled and an experimental frequency response function (FRF) for one of the eight accelerometers is shown in Figure 3. Measured modal damping was included in the FE model. Clearly, the initial model required updating to improve its correlation to the experimental FRFs.

4. PENALTY METHOD USING ANTIRESONANT FREQUENCIES

The *penalty method* was chosen as the update method for this research, because it accommodated the use of antiresonant frequencies as measured data and the use of rigid element dimensions as update parameters. The penalty method is a frequently used method for updating FE models using the sensitivities of modal data. This development of the penalty method was taken from Friswell and Mottershead's text on FE model updating [1]. The method is extended here to include antiresonant frequencies as modal data.

The penalty method is based upon a first order Taylor-series expansion that relates the differences between experimental and model eigendata ($\boldsymbol{\delta z}$) to steps in the update parameters ($\boldsymbol{\delta\theta}$). In this paper, $\boldsymbol{\delta z}$ is made up of the differences between modelled and experimental eigenvalues (λ_m and λ_e) and antiresonant eigenvalues (λ_m^a and λ_e^a), where antiresonant eigenvalues are the antiresonant frequencies squared ($\lambda^a = (\omega_n^a)^2$). Model antiresonant eigenvalues were found from an eigenanalysis of $\mathbf{M}_{pq}$ and $\mathbf{K}_{pq}$, where the subscripts p and q indicate that row p and column q are deleted from $\mathbf{M}$ and $\mathbf{K}$ [12].

The scalar penalty function to be minimized is then defined as

$$J = (\boldsymbol{\delta z} - \mathbf{S}\boldsymbol{\delta\theta})^{\mathrm{T}}\mathbf{W}_{\varepsilon\varepsilon}(\boldsymbol{\delta z} - \mathbf{S}\boldsymbol{\delta\theta}) + (\boldsymbol{\theta} - \boldsymbol{\theta}_0)^{\mathrm{T}}\mathbf{W}_{\theta\theta}(\boldsymbol{\theta} - \boldsymbol{\theta}_0), \tag{1}$$

where $\boldsymbol{\theta}_0$ are the initial update parameter values, $\mathbf{W}_{\varepsilon\varepsilon}$ is a weighting matrix on the measured eigendata and $\mathbf{W}_{\theta\theta}$ is a weighting matrix on the update parameters. The sensitivity matrix S is defined to include both eigenvalue and antiresonant eigenvalue sensitivities:

$$\mathbf{S} = \begin{bmatrix} \dfrac{\partial\lambda_1}{\partial\theta_1} & \cdots & \dfrac{\partial\lambda_1}{\partial\theta_r} \\ \vdots & \ddots & \vdots \\ \dfrac{\partial\lambda_n}{\partial\theta_1} & \cdots & \dfrac{\partial\lambda_n}{\partial\theta_r} \\ & & \\ \dfrac{\partial\lambda_1^a}{\partial\theta_1} & \cdots & \dfrac{\partial\lambda_1^a}{\partial\theta_r} \\ \vdots & \ddots & \vdots \\ \dfrac{\partial\lambda_k^a}{\partial\theta_1} & \cdots & \dfrac{\partial\lambda_k^a}{\partial\theta_r} \end{bmatrix}. \tag{2}$$

The resulting solution for the set of update parameters that minimizes the penalty function is

$$\boldsymbol{\delta\theta} = (\mathbf{S}^{\mathrm{T}}\mathbf{W}_{\varepsilon\varepsilon}\mathbf{S} + \mathbf{W}_{\theta\theta})^{-1}(\mathbf{S}^{\mathrm{T}}\mathbf{W}_{\theta\theta}\boldsymbol{\delta z} - \mathbf{W}_{\theta\theta}(\boldsymbol{\theta} - \boldsymbol{\theta}_0)). \tag{3}$$

This equation is iteratively applied, recalculating $\mathbf{S}$ at every iteration, until the update parameters converge.

The eigenvalue sensitivities required in equation (2) can be found by [13]

$$\frac{\partial\lambda_i}{\partial\theta_j} = \frac{\boldsymbol{\phi}_i^{\mathrm{T}}(\partial\mathbf{K}/\partial\theta_j - \lambda_i\,\partial\mathbf{M}/\partial\theta_j)\,\boldsymbol{\phi}_i}{\boldsymbol{\phi}_i^{\mathrm{T}}\mathbf{M}\boldsymbol{\phi}_i}, \tag{4}$$

where $\boldsymbol{\phi}_i$ are the eigenvectors of $\mathbf{M}$ and $\mathbf{K}$.

The mass and stiffness matrices sensitivities can be found by finite differencing [14]:

$$\frac{\partial\mathbf{K}}{\partial\theta_j} \approx \frac{\mathbf{K}(\boldsymbol{\theta}_{0_j} + \boldsymbol{\delta\theta}_j) - \mathbf{K}(\boldsymbol{\theta}_{0_j})}{\delta\theta_j}, \qquad \frac{\partial\mathbf{M}}{\partial\theta_j} \approx \frac{\mathbf{M}(\boldsymbol{\theta}_{0_j} + \boldsymbol{\delta\theta}_j) - \mathbf{M}(\boldsymbol{\theta}_{0_j})}{\delta\theta_j}. \tag{5, 6}$$

The antiresonant eigenvalue sensitivities required in equation (2) can be found by [13]

$$\frac{\partial\lambda_b^a}{\partial\theta_j} = \frac{\boldsymbol{\eta}\eta_b^{\mathrm{T}}(\partial\mathbf{K}_{pq}/\partial\theta_j - \lambda_b^a\,\partial\mathbf{M}_{pq}/\partial\theta_j)\,\boldsymbol{\phi}_b}{\boldsymbol{\eta}_b^{\mathrm{T}}\mathbf{M}_{pq}\boldsymbol{\phi}_b}, \tag{7}$$

where $\boldsymbol{\eta}_b$ and $\boldsymbol{\phi}_b$ are the left and right eigenvectors of $\mathbf{M}_{pq}$ and $\mathbf{K}_{pq}$ respectively.

The sensitivities of $\mathbf{K}_{pq}$ and $\mathbf{M}_{pq}$ can be obtained by simply deleting row p and column q from the sensitivities of $\mathbf{K}$ and $\mathbf{M}$ from equations (5) and (6):

$$\frac{\partial\mathbf{K}_{pq}}{\partial\theta_j} = \left[\frac{\partial\mathbf{K}}{\partial\theta_j}\right]_{pq}, \qquad \frac{\partial\mathbf{M}_{pq}}{\partial\theta_j} = \left[\frac{\partial\mathbf{M}}{\partial\theta_j}\right]_{pq}. \tag{8, 9}$$

5. FE MODEL UPDATING OF THE FTE

A program for the FE model updating method described above was created using MATLAB™. The SDT formed the initial FE model $\mathbf{M}$ and $\mathbf{K}$ matrices using initial values

TABLE 1

Final parameter values from model updating

Update parameter	Initial value	Antiresonant update	Non-antiresonant update
E_L (GPa)	70	50	50
I_{batt} (cm^4)	0·15	0·09	0·13
d_K (cm)	5·1	4·8	4·6
d_B (cm)	2·5	2·2	2·2
d_{RB} (cm)	1·3	1·1	1·2
d_{TP} (cm)	6·4	9·1	5·6
d_{MP} (cm)	6·4	9·1	6·1

for the update parameters. The SDT subspace iteration eigensolver [6] and the MATLAB™ function *eigs* [15] were used to find the eigenvalues and antiresonant eigenvalues respectively. The difference between the modelled and experimental modal data was then calculated. The sensitivities of the modal data were found from equations (4)–(9). The method then used the sensitivities to determine a step in the update parameters (equation (3)) that reduced the difference between modelled and experimental data. The FE model was reformed using the new values of the update parameters, and the process repeated until the Euclidean norm of the parameter step vector $\boldsymbol{\delta\theta}$ was less than 0·01.

The choice of update parameters is critical for successful model updating. For the FTE, the likely source of modelling error was in the joints. Therefore, five parameters were chosen to be the joint rigid element dimensions d_K, d_B, d_{RB}, d_{TP}, and d_{MP}. Model updating produced the best results when two other parameters, the longeron elastic modulus (E_L) and the batten bending moment of inertia (I_{batt}), were included as update parameters. The final set of update parameters is shown in Table 1.

Weighting matrices on the measured data and the parameter estimates were used to reflect different levels of confidence in the accuracy of the measurements and the amount of error in each update parameter. Friswell and Mottershead recommend letting the weighting matrices $\mathbf{W}_{\varepsilon\varepsilon}$ and $\mathbf{W}_{\boldsymbol{\theta\theta}}$ be diagonal matrices with their elements equal to the reciprocal of the corresponding estimated measurement and parameter variances [1]. The standard deviations of the natural frequencies and antiresonant frequencies were assumed to be 0·5 and 1% of their identified values respectively. The standard deviations of the update parameters were made 10% of their initial values for E_L and I_{batt}, 50% for d_K, d_B and d_{RB}, and 20% for d_{TP} and d_{MP}.

6. FE MODEL UPDATING RESULTS

The first update was called the antiresonant update, because it used 11 natural frequencies and 21 antiresonant frequencies from all 8 FRFs. The antiresonant update converged in five iterations taking 19·5 min on a 166 MHz Pentium PC. Updating results are shown in Table 1.

In order to evaluate the benefit of using antiresonance data in updating, another update, called the *non-antiresonant update*, was accomplished using only the 11 natural frequencies. Thus, the sensitivity matrix $\mathbf{S}$ in equation (2) was reduced from a 32×7 matrix to an 11×7 matrix. The update was initially unstable. The weighting matrix on the initial parameters, $\mathbf{W}_{\boldsymbol{\theta\theta}}$ in equation (1), had to be multiplied by 30 to get the update to converge on a set of final values for the update parameters. The instability was explained by the fact that the same

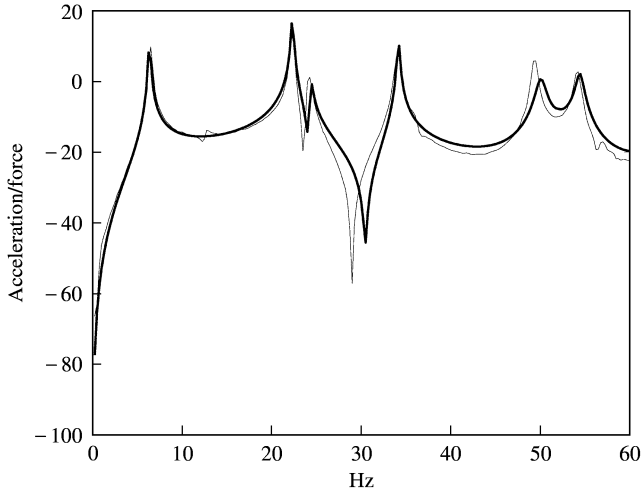

Figure 4. FRF correlation from non-antiresonant updated model: ——, modelled; ——, experimental.

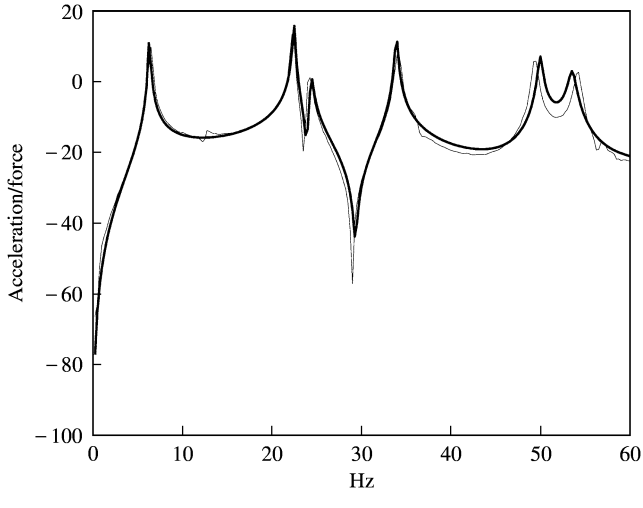

Figure 5. FRF correlation from antiresonant updated model: ——, modelled; ——, experimental.

number of unknown parameters was being solved with fewer equations. The update converged in four iterations and required 5·7 min of computation on a 166 MHz Pentium PC. The results of the update are shown in Table 1. The final non-antiresonant update parameters changed less from their initial values than in the antiresonant update, which was expected because $\mathbf{W}_{\theta\theta}$ was 30 times greater.

Both updates produced joint rigid element dimensions that were reasonable, based upon the geometry of the actual joints. However, large reductions were made to the parameters E_L and I_{batt} in both updates. The reductions in I_{batt} may be due to an error in the assumed wall thickness of the battens, since actual measurements were not taken due to the closed welded ends. The reduction in E_L is consistent with previous researchers [7, 8], and is likely due to the lack of a perfectly rigid boundary condition at the base of the FTE.

Figures 4 and 5 show an FRF from the antiresonant and non-antiresonant updated joint models. Measured modal damping was included in the FE model. The antiresonant update

TABLE 2

Cost function values

FE model	Cost function value
Initial model	76·17
Non-antiresonant updated model	13·59
Antiresonant updated model	7·03

forced greater agreement between model and experimental FRFs, especially around the antiresonant frequencies. The greatly improved antiresonance correlation suggests that the inclusion of antiresonance data, rather than the different parameter weighting matrices, was the major reason why the two updates produced different results.

Table 2 compares the initial model, the non-antiresonant updated model, and the antiresonant updated model to experimental data based on the following cost function:

$$J = \sum_{j=1}^{8} \sum_{i=1}^{400} \left(\log |\mathbf{H}_{e_{ij}}| - \log |\mathbf{H}_{m_{ij}}| \right)^2, \tag{10}$$

where $\mathbf{H}$ is a matrix whose columns are FRFs, j is the index on the eight sensor d.o.f., i is the index on the 400 frequency data points, and the subscripts e and m denote experimental and model data.

Based on Table 2, the antiresonant updated joint model produced a 48% better correlation to the experimental FRFs than the non-antiresonant updated model. Furthermore, the antiresonant update was numerically more stable than the non-antiresonant update.

7. DAMAGE DETECTION

An updated model may match the experimental data used in updating without matching other experimental data not used in updating, such as the response at higher frequencies, other sensor locations, or the responses under different structural configurations, boundary conditions, or loadings [2]. Such an updated model is not physically realistic, and the updated parameters do not necessarily correct modelling errors. For this research, the physical correctness of the antiresonant updated model was validated by using the model to predict the FRFs of damaged configurations of the FTE.

For this research, 112 possible damage states and one undamaged state were considered. The 112 damage states were broken into three categories. The first category consisted of 32 100% *damaged cases* in which one diagonal was removed from the FTE. The second category consisted of 32 50% *damaged cases* in which one diagonal had 50% the normal cross-sectional area. The third category consisted of 48 *double damaged* cases in which two diagonals were removed from the same bay.

Experimental FRFs were taken from the two driving point accelerometers at the top of the FTE. Damage cases were modelled by removing the appropriate elements from the FE model or replacing them with elements of 50% normal cross-sectional area and recalculated bending moments of inertia. Modelled driving point FRFs were then solved from the FE model of the damage cases.

The modelled FRFs for the 112 damage cases were compared to the experimental FRFs using two damage detection methods—a pattern classification method and a curve-fit

method. The first method, developed by Swenson [8] and called the pattern classifier method, applied variability to the modelled FRFs to create training data and condensed the training data into feature vectors that were plotted in 40-dimensional space. Experimental FRFs were then taken from the FTE, condensed into experimental feature vectors and plotted in 40-dimensional space. The method determined the damage case as the "nearest region" to the experimental feature vector.

The second method, developed as part of this research and called the curve-fit method, took the modelled FRFs and assembled them into a catalog of possible damage cases. Experimental FRFs were then taken from the FTE. A simple cost function was computed as the sum of squared error between the experimental FRFs and each modelled FRF in the catalog of possible damage cases. The damage was identified as the damage case with the lowest cost function. The cost function used was

$$J = \sum_{i=1}^{400} (\log|\mathbf{H}_{11_i}| - \log|\mathbf{H}_{11_i}|)^2 + \sum_{i=1}^{400} (\log|\mathbf{H}_{22_i}| - \log|\mathbf{H}_{22_i}|)^2, \tag{11}$$

where $\mathbf{H}_{11}$ and $\mathbf{H}_{22}$ are the two driving point FRFs and i is the index on the frequency data points.

8. DAMAGE DETECTION RESULTS

The pattern classification and curve-fit methods of damage detection were programmed using MATLAB™. Both damage detection methods were tested against 11 300 sets of experimental FRFs (100 for each of the 113 FTE configurations).

The curve-fit method correctly identified the damaged members in 92.6% of the tests compared to 76.1% for the pattern classification method. The breakdown in Table 3 shows where the errors in damage detection occurred.

The curve-fit method was more accurate in detecting damage than the pattern classification method. Also, it was observed that the errors made by the curve-fit method were all confined to the 50% damaged members category. Further investigation showed that the vast majority of 50% damaged cases were misidentified as other 50% damaged cases or the undamaged case. Therefore, it was concluded that the 50% damaged FRFs were too similar to each other and to the undamaged FRFs to reliably predict the damaged member.

The difficulty in accurately identifying slight damage has important implications for the practicality of fielded damage detection systems. The engineer must ensure that the damage detection system has the appropriate number and location of sensors collecting enough information to detect the desired level of damage. In the case of the FTE, the ability to

TABLE 3

Damage detection accuracy (# of cases correctly identified/# of possible cases)

Damage category	Curve-fit method	Pattern classifier method
Undamaged	1/1	1/1
50% damaged	16/32	2/32
100% damaged	32/32	31/32
Double damaged	48/48	45/48

detect slight damage cases could likely be improved by employing a method based on the shifts in the natural frequencies and antiresonant frequencies from their undamaged values. Such a method would remove the initial FE model error to first order from the damage detection process [16] and is a recommended area for further research. Utilizing more than just the two driving point FRFs would also likely improve results.

9. CONCLUSIONS

Finite element model updating using antiresonant frequencies was found to be successful in producing an accurate model of an experimental structure with complex joints. The method was also shown to produce an updated model that matched experimental FRFs 48% better than an update that used natural frequencies only. Lastly, the model updating process was observed to be more numerically stable when antiresonant frequencies were used with natural frequencies.

The fact that the curve-fit method was 100% successful in identifying all 100% damaged and double-damaged cases, using only two sensors, validated the physical correctness of the antiresonant updated model. The high quality of the model was attributed to the use of rigid elements that were updated using antiresonant frequencies. Furthermore, it was found that for this research the curve-fit method was a better damage detection method than the pattern classifier method based on the fact that it produced more accurate results, required less computation, and did not require training data.

ACKNOWLEDGMENTS

The authors would like to acknowledge the support of the Air Force Research Laboratory, Space Vehicles Directorate in this research effort as well as Captain Doug Gaeta of the Space Warfare Center for providing the experimental data.

REFERENCES

1. M. I. Friswell and J. E. Mottershead 1995 *Finite Element Model Updating and Structural Dynamics*, 158–282. Dordrecht: Kluwer.
2. J. E. Mottershead and M. I. Friswell 1993 *Journal of Sound and Vibration* **167**, 347–359. Model updating in structural dynamics: a survey.
3. D. A. Rade, G. Lallement and L. A. da Silva 1996 *Proceedings of the* 14*th IMAC*, 1078–1085. A strategy for the enrichment of experimental data as applied to an inverse eigensensitivity-based F.E. model updating method.
4. J. E. Mottershead 1998 *Proceedings of the* 16*th IMAC*, 500–503. On the zeros of structural frequency response functions and their application to model assessment and updating.
5. G. Lallement and S. Cogan 1992 *Proceedings of the* 10*th IMAC*, 487–493. Reconciliation between measured and calculated dynamic behaviors: enlargement of the knowledge space.
6. E. Balmes 1997 *Structural Dynamics Toolbox User Manual*. Paris, France: Scientific Software Group.
7. R. G. Cobb 1996 *Ph.D. Dissertation, Air Force Institute of Technology* (*AU*), *Wright-Patterson AFB OH*. Structural Damage Identification from Limited Measurement Data.
8. E. D. Swenson 1998 *MS Thesis*, *AFIT/GA/ENY*/98–01, *Air Force Institute of Technology* (*AU*), *Wright-Patterson AFB*, *OH*. Damage detection using pattern classifiers.
9. J. E. Mottershead, M. I. Friswell, G. H. T. Ng and J. A. Brandon 1996 *Mechanical Systems and Signal Processing* **10**, 171–182. Geometric parameters for finite element model updating of joints and constraints.
10. H. Ahmadian, J. Mottershead and M. Friswell 1996 *Proceedings of the* 14*th IMAC*, 591–596. Joint modelling for finite element model updating.

11. B. HORTON, H. GURGENCI, M. VEIDT and M. I. FRISWELL 1999 *Proceedings of the* 17*th IMAC*, 1556–1562. Finite element model updating of the welded joints in a tubular H-frame.
12. J. HE and Y.-Q. LI 1995 *The International Journal of Analytical and Experimental Modal Analysis* **10**, 224–235. Relocation of anti-resonances of a vibratory system by local structural changes.
13. L. C. ROGERS 1970 *American Institute of Aeronautics and Astronautics Journal* **8**, 943–944. Derivatives of eigenvalues and eigenvectors.
14. G. J. MOORE 1994 *MSC/NASTRAN Design Sensitivity and Optimization User's Manual*. Los Angeles, CA: MSC/NASTRAN.
15. Mathworks Inc. 1996 *Using Matlab Version* 5.
16. M. I. FRISWELL and J. E. T. PENNY 1997 *EUROMECH* 365 *International Workshop*: *DAMAS*, *Structural Damage using Advanced Signal Processing Procedures*, *Sheffield*, *UK*, June/July. Is damage location using vibration measurements practical?